Applied Thermal Engineering 30 (2010) 1574–1579

Contents lists available at ScienceDirect

Applied Thermal Engineering

journal homepage: www.elsevier.com/locate/apthermeng

A two-dimensional inverse heat conduction problem in estimating the fluid temperature in a pipeline

T. Lu [a], B. Liu [a], P.X. Jiang [b,*], Y.W. Zhang [b], H. Li [b]

[a] School of Mechanical and Electrical Engineering, Beijing University of Chemical Technology, Beijing 100029, China
[b] Key Laboratory for Thermal Science and Power Engineering of Ministry of Education, Department of Thermal Engineering, Tsinghua University, Beijing 100084, China

ARTICLE INFO

Article history:
Received 25 September 2009
Accepted 5 March 2010
Available online 15 March 2010

Keywords:
Inverse heat conduction problem
Temperature fluctuations
Conjugate gradient method

ABSTRACT

An inverse heat conduction problem (IHCP) was investigated in the two-dimensional section of a pipe elbow with thermal stratification to estimate the unknown transient fluid temperatures near the inner wall of the pipeline. An inverse algorithm based on the conjugate gradient method (CGM) was proposed to solve the IHCP using temperature measurements on the outer wall. In order to examine the accuracy of estimations, some comparisons have been made in this case. The temperatures obtained from the solution of the direct heat conduction problem (DHCP) using the finite element method (FEM) were pseudo-experimental input data on the outer wall for the IHCP. Comparisons of the estimated fluid temperatures with experimental fluid temperatures near the inner wall showed that the IHCP could accurately capture the actual temperature in form of the frequency of the temperature fluctuations. The analysis also showed that the IHCP needed at least 13 measurement points for the average absolute error to be dramatically reduced for the present IHCP with 37 nodes on each half of the pipe wall.

1. Introduction

The solution of inverse heat conduction problems have received considerable interest because of numerous important applications in science and engineering. Applications of the inverse problem are often found in these engineering problems involving situations in which direct measurements of temperature in a body are difficult to obtain accurate thermal quantities such as surface temperatures, heat flux distributions, heat sources, thermal conductivity and heat transfer coefficients. In a recent paper Kim et al. [1] solved an inverse heat conduction problem to estimate the surface temperature from temperature readings using the maximum entropy method. Wikstroom et al. [2] investigated an inverse problem during heat treatment processes of a steel slab to obtain the time dependent local surface temperature and heat flux with temperature measurements inside the slab. Okamoto and Li [3] designed an inverse algorithm to determine the optimal boundary heat flux distribution to obtain a unidirectional solid-liquid interface in a 2-D cavity for the design of the solidification processing systems. Ijaz et al. [4] estimated time-dependent heat flux in a two-dimensional heat conduction domain with heated and insulated walls. Aleksev [5] described the use of an inverse problem in optimum heat flux sensors development. Lee et al. [6] estimated the unknown space- and time-dependent heat source using the inverse method. Su and Neto [7] solved a two-dimensional inverse heat conduction problem to estimate strength of a volumetric heat source in a cylindrical rod. Monteau [8] solved an inverse problem to determine the thermal conductivity of sandwich bread by recording the temperature during the convection cooling process. Huang and Tsai [9] investigated a three-dimensional inverse heat conduction problem to obtain the local time-dependent surface heat transfer coefficients for plate finned-tube heat exchangers. Anderson and Paul Singh [10] calculated the effective heat transfer coefficients using an inverse method for thawing from a single impingement jet.

A variety of numerical techniques have been proposed for the solution of inverse problems including the Levenberg–Marquardt method (LMM) [11,12], the least-squares method with regularization [13], the steepest descent method (SDM) [9,14,15], the maximum entropy method (MEM) [16] the genetic algorithm (GA) [17], the network simulation method (NSM) [18], and the conjugate gradient method (CGM) [6,19–21]. The conjugate gradient method (CGM) is derived based on the perturbation principles and transforms the inverse problem into the solutions of three problems, namely, the direct, the sensitivity, and the adjoint problems. Many researchers have used the CGM to solve the inverse problem. For example, Lee et al. [6] used the CGM to estimate the unknown space and time dependent heat sources in aluminum coated

* Corresponding author. Tel.: +86 10 62772661.
E-mail address: Jiangpx@mail.tsinghua.edu.cn (P.X. Jiang).

1359-4311/$ – see front matter
doi:10.1016/j.applthermaleng.2010.03.011

tapered optical fibers for scanning near-field optical microscopy. Chen et al. [19] used the inverse algorithm to estimate the unknown space and time dependent convection heat transfer coefficients on an annular fin while knowing the temperature or strain history at measurement positions. Lin et al. [20] used an inverse algorithm based on the CGM to estimate the boundary conditions for the unsteady laminar forced convection in parallel plate channels with wall conduction effects and minimized the objective function to reduce the estimated error. Prud'homme and Nguyen [21] used the convergence and regularization properties of the CGM for the inverse heat conduction problem to calculate a time-dependent boundary heat flux.

The temperature fluctuations of the fluid near inner wall induced by thermal stratification may cause cyclical thermal stress variations and then thermal fatigue cracking of pipe walls in the piping of nuclear or chemical power plants. Therefore, accurate fluid temperature data detailing the fluctuations is essential for analysis and prediction of thermal fatigue in piping. As shown in Fig. 1, the geometry is a pipe elbow with the hot fluid on the top and the cold fluid on the bottom. The hot and cold fluids mix but produce thermal stratification in the bend of the pipe elbow, which causes fluctuations of the fluid temperature near inner wall. In the present study, an inverse algorithm based on the CGM is applied to solve the IHCP to estimate the fluid temperature near inner wall for the two-dimensional pipe located between the bend and the horizontal sections of the pipe elbow shown in Fig. 1. The solution of the IHCP was performed on the Matlab platform. First, the two-dimensional direct heat conduction problem (DHCP) was solved with the third kind of boundary conditions on both the outer and inner walls, where the experimental fluid temperature changed with time. The DHCP then gave the temperature distribution on the pipeline surface, with the temperatures of outer wall used as quasi-experimental data which were used as the input data to the IHCP. The IHCP then produced the fluid temperatures near inner wall which were compared with the experimental fluid temperature. The number of measurement points on the outer wall needed for the IHCP to give accurate result was investigated for the same model.

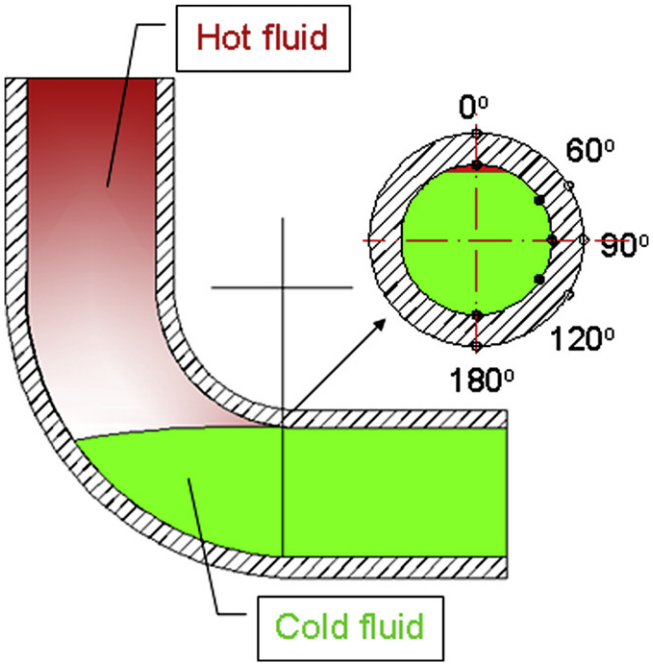

Fig. 1. The pipe elbow with thermal stratification.

2. Physical and mathematical model

2.1. Direct heat conduction problem

Fig. 2 shows the two-dimensional model of the pipeline section with an outer diameter of 60.5 mm and wall thickness of 8.7 mm. The inner and outer walls are both subjected to the convective boundary condition. The ambient temperature for the outer wall is constant, while the fluid temperature inside the pipeline changes over time as shown in Fig. 3.

The governing equations for the DHCP to calculate the transient temperature distribution $T(x,y,\tau)$ inside the pipe are:

$$\frac{\partial T}{\partial \tau} = \alpha\left(\frac{\partial^2 T}{\partial x^2}+\frac{\partial^2 T}{\partial y^2}\right)(x,y)\in\Omega \tag{1}$$

where T is the temperature, α is the thermal diffusivity of the pipe equal to $4.46\times10^{-6}\,m^2/s$, x, y, and τ are the space and time variables. The corresponding boundary conditions are

$$-\lambda\left(\frac{\partial T}{\partial n}\right)\Big|_{w,\mathrm{out}} = h_{\mathrm{out}}\left(T_{w,\mathrm{out}}-T_{\mathrm{f,out}}\right)(x,y)\in\text{outer wall} \tag{2}$$

$$-\lambda\left(\frac{\partial T}{\partial n}\right)\Big|_{w,\mathrm{in}} = h_{\mathrm{in}}\left(T_{\mathrm{f,in}}-T_{w,\mathrm{in}}\right)(x,y)\in\text{inner wall} \tag{3}$$

where λ is the thermal conductivity of the pipe equal to 19.35 W (m k), n is the direction vector normal to the boundary wall, h_{in} and h_{out} are the convection heat transfer coefficients of 2500 W/(m^2 K) and 1 W/(m^2 K) on the inner and outer walls, T_{f} is the fluid temperature, and T_{w} is the wall temperature. The subscripts in and out represent the inner and outer walls. The ambient temperature, $T_{\mathrm{f,out}}$ is 20 °C. The measurement time step, $\Delta\tau$, is 1 s and total time is 361 s.

The initial condition is

$$T(x,y,0) = T_0(x,y) \tag{4}$$

where $T_0(x,y)$ is the initial pipe temperature.

The unsteady two-dimensional DHCP consists of the governing equation, Eq. (1), the boundary conditions, Eqs. (2)–(3), and the initial condition, Eq. (4). The unsteady DHCP could be solved using the FEM in Matlab. However, the boundary condition at the inner

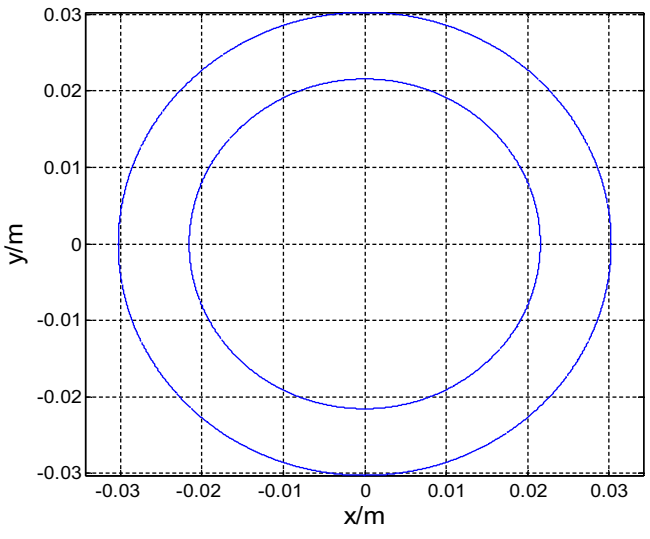

Fig. 2. Physical model.

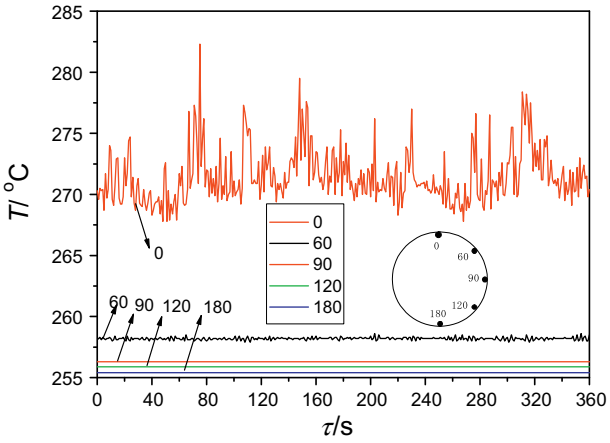

Fig. 3. Experimental fluid temperatures at five locations.

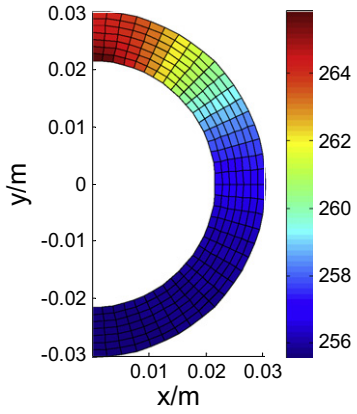

Fig. 5. Temperature field at 0 s.

wall varies with time and location. The quasi-experimental fluid temperatures near the inner wall were calculated only at five points for the symmetrical geometry in the clockwise direction at 0°, 60°, 90°, 120°, 180° from top to bottom as shown in Fig. 3. The fluid temperature at 0° is normally the highest. An approximative fluid temperature distribution near the inner wall along the circumferential direction was found using Newton interpolation with a fourth order equation. The Newton interpolation gave the fluid temperature distribution at 0 s shown in Fig. 4 as well as those at other times.

The temperature field as shown in Fig. 5 and the initial condition for the unsteady two-dimensional DHCP was obtained by solving of the steady two-dimensional DHCP using the interpolated fluid temperatures at $\tau = 0$ s. Then, the unsteady DHCP was solved using the boundary conditions using the Newton interpolation method. The results of the unsteady DHCP showed that the largest temperature fluctuations in the pipe occur at 0° on the inner wall as shown in Fig. 6. The temperature fluctuations gradually attenuate in both amplitude and frequency from the fluid to the outer wall as shown in Figs. 3 and 6.

The DHCP are then used as quasi-experimental data with the outer wall temperatures from the DHCP used as the input data to the IHCP to estimate the fluid temperatures near inner wall. The estimated fluid temperatures from the IHCP are compared with the experimental fluid value near the inner wall to evaluate the inverse algorithm for the solution of the IHCP.

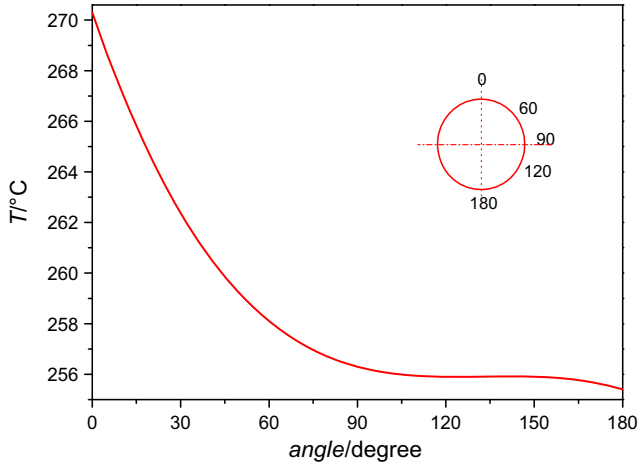

Fig. 4. Fluid temperature distributions obtained from the five selected points using Newton interpolation at 0 s.

2.2. Inverse problem

The boundary conditions and the initial condition for the DHCP were used to determine the temperature distributions in the pipe walls. The pseudo-temperatures on the outer wall were then used as input data to the IHCP to estimate the unknown fluid temperature fluctuations near the inner wall. The fluid temperatures near the inner wall were then calculated using the IHCP with the CGM. The predicted fluid temperatures near inner wall were then compared with the experimental value to evaluate the IHCP.

During the IHCP solution process, the direct heat conduction problem is repeatedly solved using various wall temperature distributions to calculate the outer wall temperature which is compared with the input outer wall temperature. Generally, an IHCP can be treated as an optimization problem. The unknown fluid temperature near inner wall is estimated from knowledge of the input outer wall temperature using an objective function based on the least-squares method which is minimized with the CGM:

$$\min J = \frac{1}{2}\sum_{m=1}^{M}\sum_{n=1}^{N}\left[T_{\mathrm{Est},m,n} - T_{\mathrm{Exp},m,n}\right]^2 \tag{5}$$

where $T_{\mathrm{Est},m,n}$ is the estimated outer wall temperature from the IHCP, $T_{\mathrm{Exp},m,n}$ is the input outer wall temperature from the early

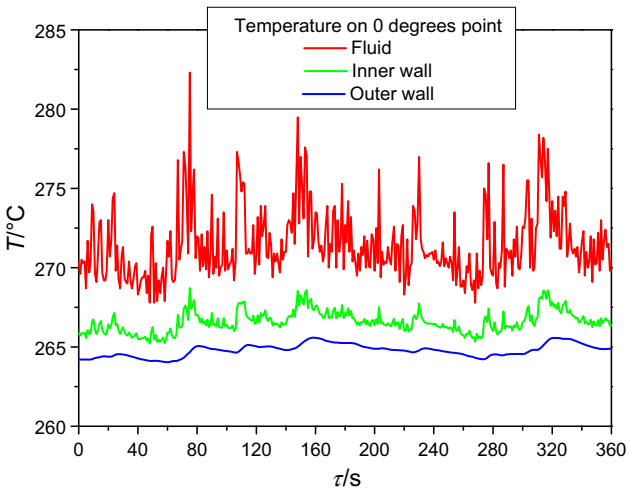

Fig. 6. Temperature fluctuations at the top of the pipe.

DHCP results, m denotes the number of measurement points on outer wall and n denotes the number of time steps. The consistency between the input data and the estimated data acts as a constraint on the optimization problem.

The CGM was used to estimate the unknown inner wall temperatures using the iterative process

$$T^{b+1}_{f,k,n} = T^{b}_{f,k,n} - \beta^b d^b_{k,n} \tag{6}$$

where b denotes the number of iterations, k denotes the node index for the inner wall, $T_{f,k,n}$ is the fluid temperature near inner wall, β^b is the step size, and $d^b_{k,n}$ is the search direction given by

$$d^b_{k,n} = \left(\frac{\partial J}{\partial T_{f,k,n}}\right)^b + \gamma^b d^{b-1}_{k,n} \tag{7}$$

where $\partial J/\partial T_{f,k,n}$ is the gradient of the objective function. The conjugate coefficient, γ^b, is determined by

$$\gamma^b = \frac{\sum_{k=1}^{K}\sum_{n=1}^{N}\left[\left(\frac{\partial J}{\partial T_{f,k,n}}\right)^b\right]^2}{\sum_{k=1}^{K}\sum_{n=1}^{N}\left[\left(\frac{\partial J}{\partial T_{f,k,n}}\right)^{b-1}\right]^2} \text{ with } \gamma^0 = 0. \tag{8}$$

The step size β^b is

$$\beta^b = \frac{\sum_{j=1}^{M}\sum_{i=1}^{N}(T_{Est,j,i} - T_{Exp,j,i})\sum_{k=1}^{K}\sum_{n=1}^{N}\left(\frac{\partial T_{j,i}}{\partial T_{f,k,n}}\right)^b d^b_{k,n}}{\sum_{j=1}^{M}\sum_{i=1}^{N}\sum_{k=1}^{K}\sum_{n=1}^{N}\left[\left(\frac{\partial T_{j,i}}{\partial T_{f,k,n}}\right)^b d^b_{k,n}\right]^2} \tag{9}$$

where $\partial T_{j,i}/\partial T_{f,k,n}$ is the sensitivity coefficient. The sensitivity coefficient is calculated by differentiating the direct problem in Eqs. (1)–(4) with respect to $T_{f,k,n}$. In the following equations, we mark the sensitivity coefficient as $\theta(x,y;\tau) = \partial T(x,y;\tau)/\partial T_{f,k,n}$.

$$\frac{\partial}{\partial\tau}\theta(x,y;\tau) = \alpha\left[\frac{\partial^2}{\partial x^2}\theta(x,y;\tau) + \frac{\partial^2}{\partial y^2}\theta(x,y;\tau)\right] \quad (x,y)\in\Omega \tag{10}$$

$$-\lambda\frac{\partial}{\partial n}\theta_w(x,y;\tau) = h_{out}\theta_w(x,y;\tau) \quad (x,y)\in \text{outer wall} \tag{11}$$

$$-\lambda\frac{\partial}{\partial}\theta_w(x,y;\tau) = h_{in}\psi(k',n') \quad (x,y)\in \text{inner wall} \tag{12}$$

for $k' = 1,2,\cdots K; n' = 1,2,\cdots N$, where

$$\begin{cases} \text{if } k'=k,\ n'=n & \psi(k,n)=1 \\ \text{otherwise} & \psi(k,n)=0 \end{cases} \tag{13}$$

$$\theta(x,y;0) = 0 \quad (x,y)\in\Omega \tag{14}$$

The gradient of the objective function, $\partial J/\partial T_{f,k,n}$ is determined by differentiating Eq. (5) with respect to $T_{f,k,n}$ to obtain

$$\frac{\partial J}{\partial T_{f,k,n}} = \sum_{j=1}^{M}\sum_{i=1}^{N}(T_{Est,j,i} - T_{Exp,j,i})\frac{\partial T_{j,i}}{\partial T_{f,k,n}} \tag{15}$$

The convergence condition for the minimization is

$$\left|J\left(T^b_{f,k,n}\right) - J\left(T^{b-1}_{f,k,n}\right)\right| < \mu \tag{16}$$

where μ is a small positive number used as the stopping criterion.

The computational procedure for the solution of the inverse heat conduction problem is summarized as follows.

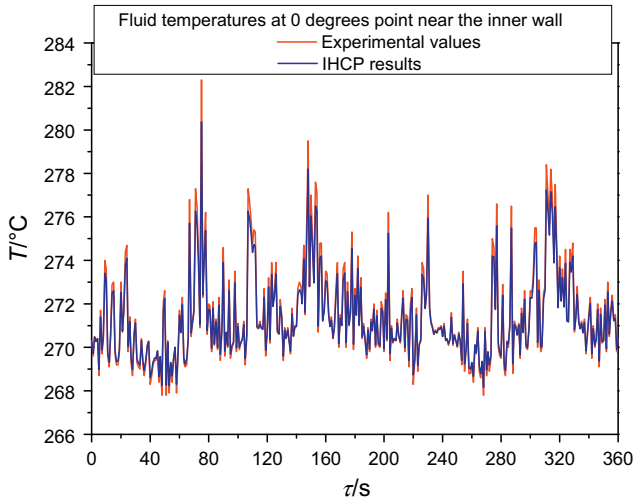

Fig. 7. Comparison of fluid temperatures estimated by the IHCP with the experimental temperatures at 0° near the inner wall from 0 s to 360 s.

Step 1. Set an initial T^0_f and solve the sensitivity problem from Eqs. (10)–(14) to calculate the sensitivity coefficient $\partial T_{m,n}/\partial T_{f,k,n}$.
Step 2. Solve the direct problem to obtain the fluid temperatures near inner wall, $T_{f,k,n}$, from Eqs. (1)–(4).
Step 3. Calculate the objective function a Eq. (5) to obtain J. Terminate the iteration process if the specified stopping criterion is satisfied to obtain the optimized $T^b_{f,k,n}$, otherwise go to step 4.
Step 4. Calculate the gradient of the objective function $\partial J/\partial T_{f,k,n}$.
Step 5. Calculate the conjugate coefficient, γ^b, the research direction, $d^b_{k,n}$, and the step size, β^b.
Step 6. Calculate $T^{b+1}_{,k,n}$, $T^{b+1}_{,k,n} = T^b_{,k,n} - \beta^b d^b_{k,n}$, set $b = b+1$, and go to step 2.

3. Results and discussion

The IHCP was solved with temperatures on the outer wall obtained from the DHCP results to estimate the fluid temperatures near inner wall. The mesh included 296 elements with 37 nodes along half of both the inner and outer walls. The 37 nodes on the

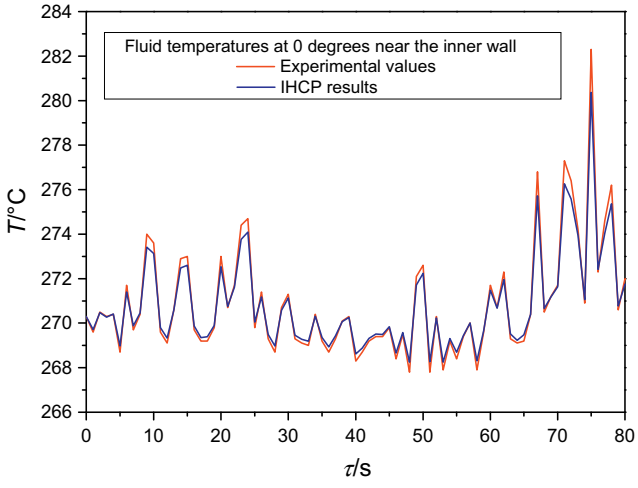

Fig. 8. Comparison of fluid temperatures estimated by the IHCP with the experimental temperatures at 0° near the inner wall from 0 s to 80 s.

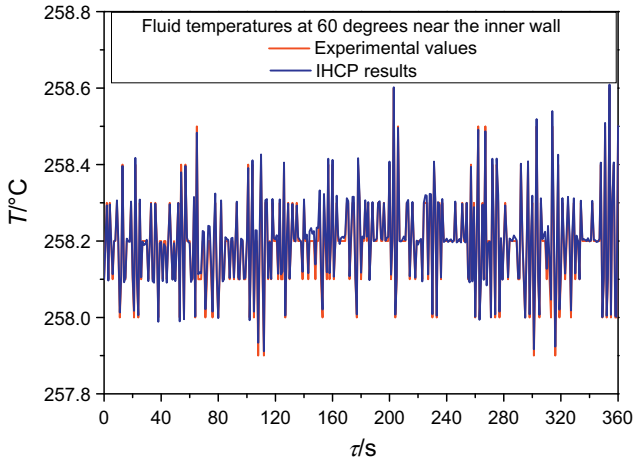

Fig. 9. Comparison of fluid temperatures estimated by the IHCP with the experimental temperatures at 60° near the inner wall from 0 s to 360 s.

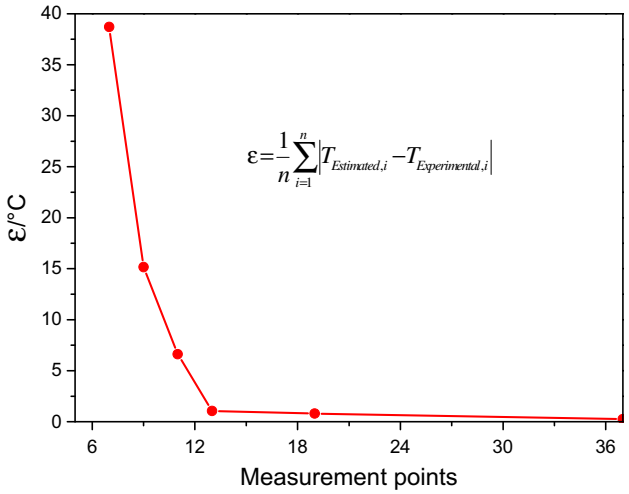

Fig. 11. Average absolute errors for various number of measurement points.

half of the outer wall were used as the input points to the IHCP. The calculation required 2000 iterations and about 6 h of computational time on a PC with Intel(R) Core(TM) 2 Quad 2.4 GHz processor.

The estimated temperatures from the IHCP are compared with the experimental fluid temperatures at top (0°) near inner wall in Fig. 7 from 0 to 360 s. The temperatures estimated by the IHCP agree well with the experiment value with an average absolute error of 0.255 °C. The maximum discrepancy in estimated fluid temperatures near inner wall is 0.68% at 75 s because of the most sharp temperature fluctuation. Fig. 8 amplifies Fig. 7 from 0 s to 80 s to clearly show the differences between the two results. The result shows that the IHCP can accurately capture the amplitudes and frequencies of temperature fluctuations produced by the DHCP.

The fluid temperatures estimated by the IHCP were compared with the experimental temperatures at 60° on the inner wall in Fig. 9 from 0 to 360 s. The temperatures estimated by the IHCP at 60° agree even better with the experimental value than the temperature in Figs. 7 and 8 for 0° with a smaller average absolute error of 0.010 °C and a smaller maximum discrepancy of 0.02% at 313 s. The better agreement at 60° is due to the smaller fluctuation amplitudes of fluid temperature at 60° than at 0° as shown in Fig. 3. The comparison at 90°, 120°, and 180° are even better than those at 60°. The number of measurement points needed on the outer wall to give accurate results was evaluated by using different number of measurement points for the IHCP. Six different cases were considered. Firstly, the DHCP was solved with a fine mesh with 37 nodes on both the inner and outer walls to obtain 37 temperature data points on the outer wall, which is needed as the pseudo-experimental data. Then, 7 to 19 points were chosen on a uniform distribution in the clockwise direction as the input data to the IHCP to simulate a limited number of actual measurement points. However, the IHCP required 37 points on the half of the outer wall used in the analysis. The data points were interpolated with the piecewise cubic spline interpolation to get 37 points on the outer wall.

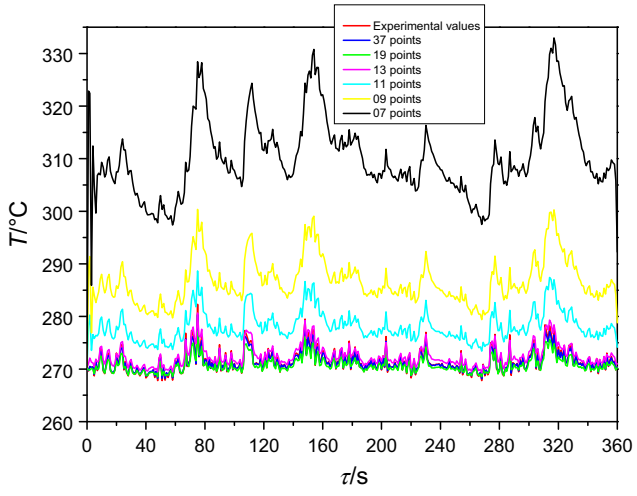

Fig. 10. Comparison of the IHCP results with the experimental values for various of measurement points.

Only the estimated fluid temperatures at 0° near the inner wall are shown in Fig. 10 for the various number of measurement points on the outer wall because temperatures of this point fluctuated most heavily. The result shows that the deviations increase gradually with decreasing number of the measurement points, which is due to the increasing error of the interpolating. The average absolute errors between the IHCP results and the DHCP results are shown in Fig. 11. When the number of measurement points is more than 13, the average absolute error decreases dramatically, as concludes that at least 13 measurement points should be chosen to achieve reliable results for the IHCP in this case.

4. Conclusions

An inverse two-dimensional thermal conduction heat transfer analysis was developed in Matlab using the conjugate gradient method. The analysis shown that

(1) an algorithm based on the CGM can be applied to solve the inverse thermal conduction problem to estimate the unknown transient fluid temperatures near the inner wall of the pipeline with thermal stratification;
(2) the unknown fluid temperatures near the inner wall were accurately obtained by solving the IHCP with the outer wall temperature measurements. The DHCP was solved in Matlab to obtain the temperature distributions on the outer wall with these then used as pseudo-experimental values. The IHCP was solved using the CGM with the temperatures on the outer

surface from the DHCP used as the input pseudo-experimental data to the IHCP to estimate the fluid temperatures near the inner wall. Comparison of the fluid temperatures estimated by the IHCP with the experimental value showed that the unknown fluid temperatures near the inner wall can be accurately estimated with both the amplitudes and frequency of the temperature fluctuation accurately produced;

(3) analysis of the number of measurement points needed on outer wall showed that the IHCP results with more than 13 measurement points on the outer wall were more reliable for the present case with 37 nodes on the mesh on each half of each wall.

Acknowledgements

This work was supported by a project of the Beijing Novel Program (No. 2008B16).

References

[1] K.K. Sun, B.S. Jung, W.I. Lee, An inverse estimation of surface temperature using the maximum entropy method. International Communication of Heat and Mass Transfer 34 (2007) 37–44.
[2] P. Wikstrom, W. Blasiak, F. Berntsson, Estimation of the transient surface temperature and heat flux of a steel slab using an inverse method. Applied Thermal Engineering 27 (2007) 2463–2472.
[3] K. Okamoto, B.Q. Li, A regularization method for the inverse design of solidification processes with natural convection. International Journal of Heat and Mass Transfer 50 (2007) 4409–4423.
[4] U.Z. Ijaz, A.K. Khambampati, M.-C. Kim, S. Kim, K.-Y. Kim, Estimation of time-dependent heat flux and measurement bias in two-dimensional inverse heat conduction problems. International Journal of Heat and Mass Transfer 50 (2007) 4117–4130.
[5] A.K. Alekseev, The heat flux measurement method based on isotherm registration. International Journal of Heat and Mass Transfer 40 (1997) 1643–1646.
[6] H.-L. Lee, W.-J. Chang, W.-L. Chen, Y.-C. Yang, An inverse problem of estimating the heat source in tapered optical fibers for scanning near-field optical microscopy. Ultramicroscopy 107 (2007) 656–662.
[7] J. Su, A.J. Silva Neto, Two-dimensional inverse heat conduction problems of source strength estimation in cylindrical rods. Applied Mathematical Modelling 25 (2001) 861–872.
[8] J.-Y. Monteau, Estimation of thermal conductivity of sandwich bread using an inverse method. Journal of Food Engineering 85 (2008) 132–140.
[9] C.-H. Huang, Y.-L. Tsai, A transient 3-D inverse problem in imaging the time-dependent local heat transfer coefficients for plate fin. Applied Thermal Engineering 25 (2005) 2478–2495.
[10] B.A. Anderson, R. Paul Singh, Effective heat transfer coefficient measurement during air impingement thawing using an inverse method. International Journal of Refrigeration 29 (2006) 281–293.
[11] L.B. Dantas, H.R.B. Orlande, R.M. Cotta, An inverse problem of parameter estimation for heat and mass transfer in capillary porous media. International Journal of Heat and Mass Transfer 46 (2003) 1587–1598.
[12] W.M. Brasil, J. Su, A.P. Silva Freire, An inverse problem for the estimation of upstream velocity profiles in an incompressible turbulent boundary layer. International Journal of Heat and Mass Transfer 47 (2004) 1267–1274.
[13] J.I. Frankel, Residual-minimization least-squares method for inverse heat conduction. Computers and Mathematics with Applications 32 (1996) 117–130.
[14] C.-H. Huang, C.-A. Chen, A three-dimensional inverse geometry problem in estimating the space and time-dependent shape of an irregular internal cavity. International Journal of Heat and Mass Transfer 52 (2009) 2079–2091.
[15] C.-H. Huang, L.-C. Jan, R. Li, A.J. Shih, A three-dimensional inverse problem in estimating the applied heat flux of a titanium drilling – theoretical and experimental studies. International Journal of Heat and Mass Transfer 50 (2007) 3265–3277.
[16] S.K. Kim, W.I. Lee, Solution of inverse heat conduction problems using maximum entropy method. International Journal of Heat and Mass Transfer 45 (2002) 381–391.
[17] H.Y. Li, C.Y. Yang, A genetic algorithm for inverse radiation problems. International Journal of Heat and Mass Transfer 40 (1997) 1545–1549.
[18] J. Zueco, F. Alhama, C.F. Gonzalez-Fernandez, Inverse determination of temperature dependent thermal conductivity using network simulation method. Journal of Materials Processing Technology 174 (2006) 137–144.
[19] W.-L. Chen, Y.-C. Yang, H.-L. Lee, Inverse problem in determining convection heat transfer coefficient of an annular fin. Energy Conversion and Management 48 (2007) 1081–1088.
[20] D.T.W. Lin, W.-M. Yan, H.-Y. Li, Inverse problem of unsteady conjugated forced convection in parallel plate channels. International Journal of Heat and Mass Transfer 51 (2008) 993–1002.
[21] M. Prud'homme, T.H. Nguyen, On the iterative regularization of inverse heat conduction problems by conjugate gradient method. International Communication of Heat and Mass Transfer 25 (1998) 999–1008.